CYCLIC BEHAVIOR OF A RESTRAINED STEEL BRACE UNDER AXIAL LOADING

by Minoru WAKABAYASHI[I], Chiaki MATSUI[II] and Isao MITANI[III]

SINOPSIS In order to clarify the effects of end restraints on the cyclic behavior of braces, steel bars restrained against rotation at both ends were tested under alternating axial load, the slenderness ratio and stiffness of end restraints being varied. It is shown that the approximate analysis predicts the experimental behavior sufficiently well. It is concluded that important parameters representing the resistantce of the brace against the earthquake motion can be estimated by the proposed empirical formulas, when the effective slenderness ratio of the brace is given.

INTRODUCTION It has been well recognized that the hysteretic elastic-plastic behavior of a braced frame under earthquake motion is significantly affected by that of braces themselves, and thus it is essential to clarify the behavior of a brace under repeated tension and compression. Some experimental and theoretical studies have been reported on cyclic behavior of braces simply supported at both ends[1,2]. In actual steel frames, braces are rigidly or semi-rigidly connected to frame member, and therefore restrained against rotation at both ends rather than simply supported. In addition, initial crookedness and unavoidable eccentricity of load exist. Very few studies are found on influence of restraint at bar ends and eccentricity of load on the behavior of a brace[3,4].

In order to investigate the cyclic behavior of a restrained brace under eccentrical axial load, an experiment was carried out using small-sized specimens elastically restrained at both ends against rotation. Experimental results were compared with those of analysis based on the differential equation for the elastic bending of axially loaded member and commonly adopted yield conditions.

TESTS Test program consists of two sets; twenty one specimens having square cross section, and eight specimens having H-shape cross section. All specimens were manufactured by shaping SS41 mild steel sheet, details being shown in Fig.1. Table 1 shows the names of specimens and actual values of the following parameters involved in the tests; ℓ/i, e and ℓ/ℓ_k, where ℓ denotes the member length, i the radius of gyration about the strong axis of the cross section, e the eccentricity of load, and ℓ_k the effective length depending on the end restraints. The value of e was taken equal to zero or $i/20+\ell/500$. Mechanical properties of steel material used are shown in Table 2.

Figure 2 shows the loading arrangement. End pin supports are the same as the ones in Ref.1. Restraints against rotation are provided by two springs located in the distance d from the center of rotation. The loading program was as shown in Fig. 3. The amplitudes of relative axial displacement were ±0.5, ±1.0, ±1.5 and ±2.0% of the length ℓ.

Some of the relations between N/Ny and $\Delta\ell/\ell$ obtained from the tests are shown by solid lines in Figs. 4(a)-(f), where $\Delta\ell$ is relative axial displacement, and Ny the yield axial load. Dashed lines in Fig. 4 indicate that the proper test data could not be obtained due to the rapid decrease of the load during the virgin compression. For specimens with H-shape cross section

I Prof., Disaster Prevention Research Institute, Kyoto Univ., Kyoto, Japan.
II Assoc. Prof., Faculty of Engineering, Kyushu Univ., Fukuoka, Japan.
III Lecturer, Faculty of Engineering, Kagoshima Univ., Kagoshima, Japan.

restrained at both ends. The out-of-plane deflection was observed to be excessive.

THEORETICAL ANALYSIS The model analysed in this study is a bar of length ℓ restrained at both ends by rotational springs of stiffness K and subjected to axial force N with eccentricity e, as shown in Fig. 5(a). The coordinate system is taken such that the positive x-axis is along the longitudinal axis of the bar with the origin at the left hand support, and y coincides with the principal axis of the cross section. The bar deflects in the symmetrical manner about the center, and a free body diagram of half bar is shown in Fig. 5(b), where θ_A and θ_B denote the slopes of the deflected bar at the center and the end, respectively, θ_A^p and θ_B^p the plastic rotations at the center and the end, respectively, and θ_S the rotations of the rigid bar connecting the bar with springs. Note that $\theta_A=\theta_A^p$ and $\theta_S=\theta_B-\theta_B^p$. The bar is subjected to Me+Ms at the support and M_A at the center, where Me and Ms denote the moment due to eccentricity of load and the restraining moment by the spring, respectively. The positive directions of axial force, bending moment, deflection and end slope are shown in Fig. 5(b).

The following assumptions are employed in the analysis: Square of the slope is negligibly small in comparison with unity; change in the length of the bar is small in comparison with the original length; the moment-thrust-curvature relation of the cross section is elastic-perfectly plastic; the bar must deflect when the absolute value of compression load reaches the smaller of Euler load or the yield load Ny.

The differential equation governing the deflection y of the bar shown in Fig. 5(b) is given by

$$y''-(N\cdot y)/(EI)+(Me+Ms)/(EI)=0 \qquad (1)$$

where EI denotes the flexural rigidity of the bar, and (') indicates the derivative with respect to x. The general solution of Eq.(1) is

$$y=C_1\cosh kx+C_2\sinh kx+(Me+Ms)/N \quad \text{for } N>0 \qquad (2a)$$

$$y=\bar{C}_1\cos kx+\bar{C}_2\sin kx+(Me+Ms)/N \quad \text{for } N<0 \qquad (2b)$$

where Ci and $\bar{C}i$ are constants of integration, and $k^2=|N|/EI$.

Boundary conditions to determine the value of Ci and $\bar{C}i$ are as follows:

$$\text{At } x=0 \;;\; y=0 \quad \text{and at} \quad x=\ell/2 \;;\; y=y_m \qquad (3a,b)$$

where y_m denotes the deflection at the center of the bar.
When the plastic hinge does not appear at the support, Ms is given by

$$Ms=-K\cdot\theta s=-K\cdot(y'|_{x=0}-\theta_B^p) \qquad (4)$$

where the value of θ_B^p is determined from the initial condition of the loading history. When the plastic hinge forms at the support, the member end moment must satisfy the yield condition, and thus,

$$Ms=\delta\cdot Mpc-Me \qquad (5)$$

where Mpc is the reduced full plastic moment due to axial thrust, and δ is taken equal to 1 if N>0 and to -1 if N<0. Me is simply given by $Me=N\cdot e$.

The deflection y finally contains unknowns y_m and N. The relation between y_m and N is obtained from the following conditions When the yield condition is not satiafied at the center,

$$y'|_{x=\frac{\ell}{2}}=\theta_A^p=\text{constant}. \qquad (6)$$

must be satisfied, where the actual value of θ_A^p is again given from the initial condition of the loading history. On the other hand, when the yield condition is satisfied at the center,

$$EI\cdot y''|_{x=\frac{\ell}{2}}=-\delta\cdot Mpc \qquad (7)$$

must be satisfied. Therefore, the value of the one of unknowns y_m and N can

be numerically determined according to the assumed value of the other.

The relative axial displacement $\Delta\ell$ can be decomposed to four components [2],

$$\Delta\ell = \Delta\ell_e + \Delta\ell_g + \Delta\ell_p + \Delta\ell t \qquad (8)$$

The first two terms in the right hand side of Eq.(8) are given by

$$\Delta\ell_e = N \cdot \ell/(EA) \quad , \quad \Delta\ell_g = -\frac{1}{2}\int_0^{\ell}(y')^2 dx \qquad (9a,b)$$

and $\Delta\ell t$ is due to plastic elongation distributed along the bar axis which appears only under pure tention. With dots denoting the rates, the relation

$$\dot{\Delta\ell}_p = \frac{\partial\Phi/\partial N}{\partial\Phi/\partial M} \cdot \dot{\theta}^p \qquad (10)$$

can be derived from the flow rule, where Φ is the yield function and θ^p is the plastic rotation at the plastic hinge. Assuming that the relation by Eq. (10) is piece-wise linear, the value of $\Delta\ell_p$ is obtained by integrating Eq. (10) numerically.

Analytical behavior of specimens are shown by dashed lines in Figs. 4 (a)-(f). Since the out-of-plane deflection was observed excessively for the case of restrained bars with H-shape cross section, as stated before, the analysis of these bars was carried out by assuming that the bar is fixed at both ends and buckles about the weak axis under centrical loading.

DISCUSSIONS Load-Displacement Curves Owing to end restraints, plastic hinges form both at the center and ends at different loading stages, which makes two kinks appear on the load-displacement curves in the region where the load increases gradually toward the tensile yield load, after it is reversed from compression to tention. This can be observed also in the region after the maximum compressive load is attained. Observe that only one kink appears for the case of simply supported bar. The analysis well predicts the experimental behavior.

Effects of Restraints It seems that the cyclic behavior of a brace can be characterized by the following quantities: Absolute value of compression load at the minimum axial displacement, N_Δ; maximum tension load, N_t; absolute value of maximum compression load, N_c; area of a loop, ΔW.

In Figs. 6,7,8 and 9, the values of N_Δ/N_y, N_t/N_y, N_c/N_y and $\Delta W/(N_y \cdot \ell \cdot \varepsilon_y)$ are plotted against common arguments of $\mu = \ell_k\sqrt{\varepsilon_y}/(i \cdot \pi)$ for various values of ℓ/ℓ_k, respectively, where ε_y denotes the yield strain. The values of ℓ_k of H-shape specimens(marked * in Figs. 6-9) are computed for bars fixed at both ends buckling about weak axis, based on the observation in the tests. The values of N_Δ, N_t, N_c and ΔW are taken from the fourth loop experimentally obtained at amplitude $\Delta\ell/\ell = \pm 0.5\%$. It can be observed that the relation between g and μ for $\ell/\ell_k = 1$ may be approximated in the form.

$$g = \frac{A}{\mu - 10\frac{\sqrt{\varepsilon_y}}{\pi}} + B \qquad (11)$$

where g may be taken equal to N_Δ/N_y, N_t/N_y, N_c/N_y or $\Delta W/(N_y \cdot \ell \cdot \varepsilon_y)$. The value of B is first taken equal to 0.5 for N_t/N_y-μ relation, and otherwise to 0, by inspection. Four values of A are determined by the least squares from the data plotted in Figs.6-9. In the similar manner, other sets of A values are obtained from the data for the amplitude of ± 1.0, ± 1.5 and $\pm 2.0\%$. The values of A determined in such a way are plotted against arguments of the amplitude for various cases of g in Fig. 10. And then, the relation between A and amplitude $\Delta\ell/\ell$ are approximate by the least squares as shown by four

different curves in Fig. 10, corresponding to four cases of g. The solid curves corresponding to $\ell/\ell_k=1$ and $\Delta\ell/\ell=\pm0.5\%$, shown in Figs. 6-9, are drawn using Eq.(11) in view of the value of A approximated in Fig. 10.

It is observed that $N_\Delta/Ny-\mu$, $Nt/Ny-\mu$, $Nc/Ny-\mu$ and $\Delta W/(Ny\cdot\ell\cdot\varepsilon_y)-\mu$ relations for the other values of ℓ/ℓ_k can be approximated again by hyperbolic functions of μ, similar to Eq.(11). The effects of end restraints are already considered when to evaluate the value of ℓ_k. However, as seen in Figs. 6-9 the values of N_Δ, Nt, Nc and ΔW for a specimen with end restraints are larger than those of a simply supported specimen given by Eq.(11), although both specimens have an identical value of $\ell_k\cdot\sqrt{\varepsilon_y}/(i\cdot\pi)$. Thus, introducing a magnification factor α to take this fact into account, the formula

$$f = \alpha\cdot g \qquad (12)$$

is assumed in this study, where f may be taken equal to N_Δ/Ny, Nt/Ny, Nc/Ny and $\Delta W/(Ny\cdot\ell\cdot\varepsilon_y)$ for $\ell/\ell_k=\sqrt{2}$ and $\sqrt{3}$. The values of α determined by the least squares from the test data for various values of the displacement amplitudes are plotted against arguments of ℓ/ℓ_k in Fig. 11 The relation between α and ℓ/ℓ_k can be approximated by a straight line for each case shown in Fig. 11. Note that magnification factor α is equal to 1 when $\ell/\ell_k=1$ and 2(both end fixed), the latter being physically explained by the fact that tha behavior of the simply supported bar of length $\ell/2$ is identical to the one of length ℓ fixed at both ends. The dashed and dash-dotted lines in Figs. 6-9 are drawn in view of Eq.(12) based on the approximate linear relation between α and ℓ/ℓ_k shown in Fig.(11).

Effect of Eccentricity and Shapes of Cross Section Specimens RE1200, RE1201 and RE1202 were tested under the largest eccentricity of load. Axial load-displacement curves of specimens RE1200 and RE1201 are shown as solid lines in Figs. 12(a) and (b), respectively, together with those of RC1200 and RC1201 drawn by dotted lines, which are subjected to centrical loading. A definite statement about the effect of the eccentricity can not be drawn from these test data, expect for difference in the maximum compression load attained in the initiate loading. Test results in Figs. 6-9 vary with the shapes of the cross section due to differences in yield functions and in the effect of strain hardening.

CONCLUSIONS It has been shown from the present experimental study that the effect of end restraints on the hysteretic behavior of braces is totally evaluated by the magnification factor α. In order to predict the post-buckling hysteretic behavior of a brace involved in actual braces frames, μ is first evaluated from ℓ_k in which the end restraints should be considered. Then, the value of α is taken from Fig. 11, and the values of factors considered to characterize the hysteretic behavior, i.e., N_Δ, Nt, Nc and ΔW, can be determined from Eqs. (11) and (12).

REFERENCES

1. Shibata, M., et al. : ELASTIC PLASTIC BEHAVIOR OF STEEL BRACES UNDER REPEATED AXIAL LOADING, Proc.5th WCEE, Rome, Vol.1, June 1973, pp.845-848.
2. Nonaka, T. : AN ELASTIC-PLASTIC ANALYSIS OF A BAR UNDER REPEATED AXIAL LOADING, Int. Jour. Solids and Struc., Vol.9, No.5, May 1973, pp. 569-580.
3. Fujimoto, M., et al. : STRUCTURAL CHARACTERISTICS OF ECCENTRIC K-BRACED FRAMES, Trans. Architec. Inst. of Japan, No.195, May 1972, pp. 39-49.
4. Wakabayashi, M., et al. : STUDY ON THE BEHAVIOR OF BRACES INVOLVED IN FRAMES, Proc. Annual Meeting of Architec. Inst. of Japan, Oct. 1974, pp. 965-966, and Oct. 1975, pp. 865-866.

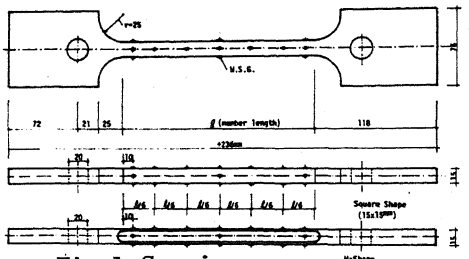

Fig.1 Specimen

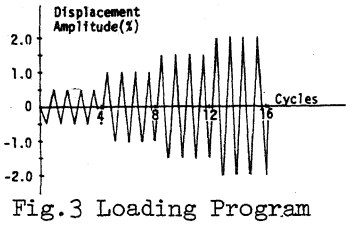

Fig.3 Loading Program

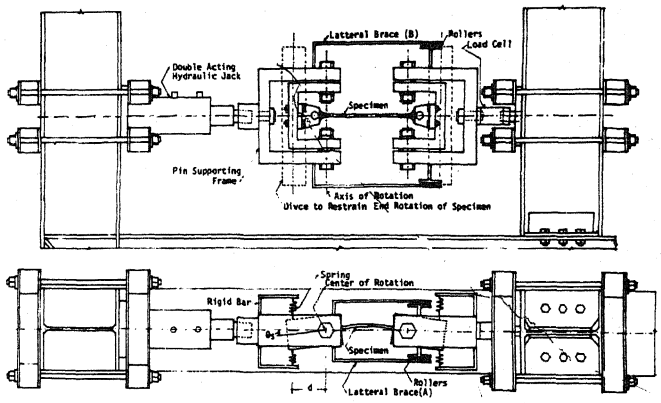

Fig.2 Loading Arrangement

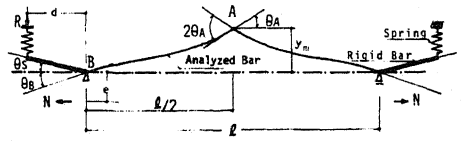

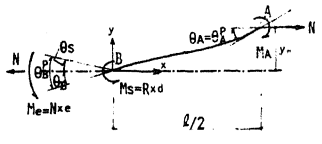

Fig.5 Model for Analysis

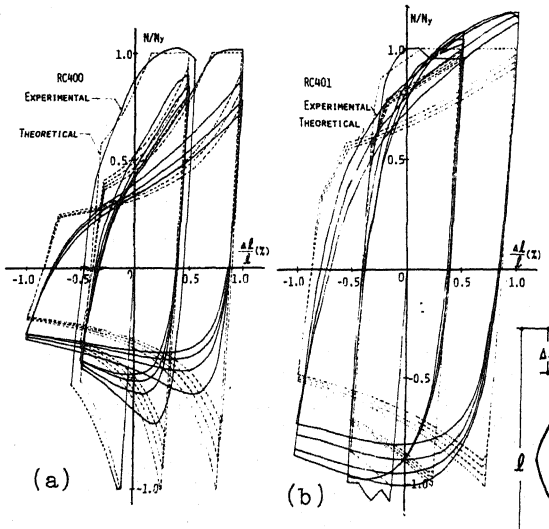

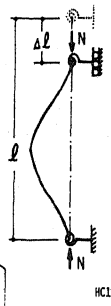

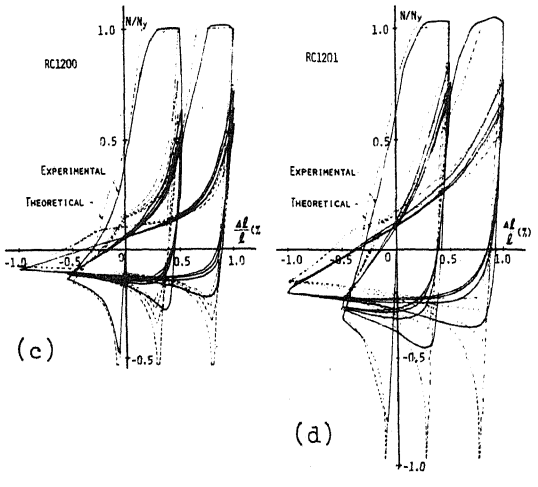

Fig.4 Axial Load-Displacement Relations

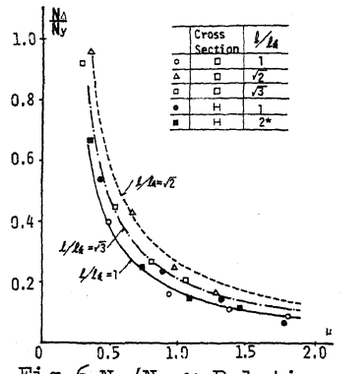

Fig.6 N_Δ/N_y-μ Relations

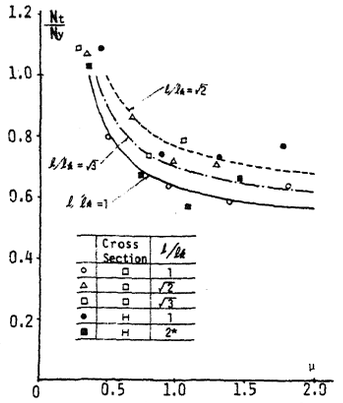

Fig.7 N_t/N_y-μ Relations

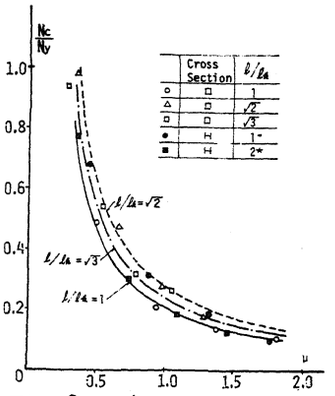

Fig.8 N_c/N_y-μ Relations

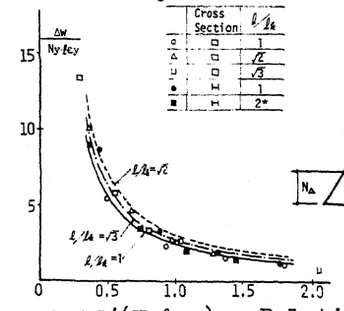

Fig.9 $\Delta W/(N_y \ell \varepsilon_y)$-μ Relations

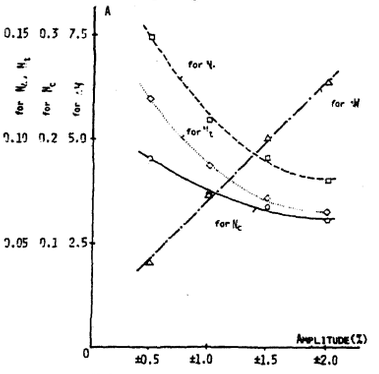

Fig.10 Values of A

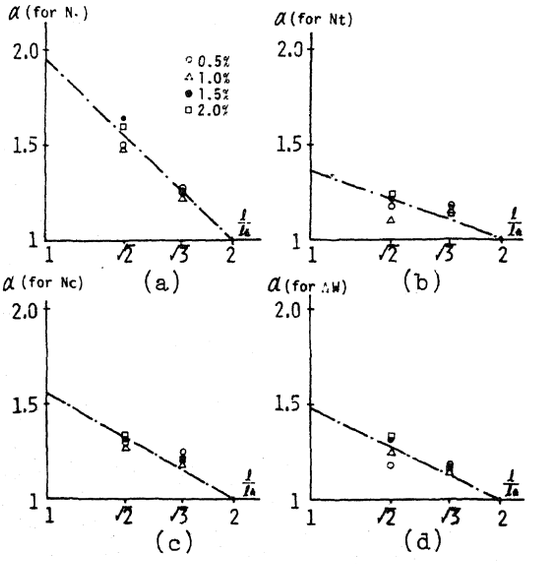

Fig.11 α-ℓ/ℓ_K Relations

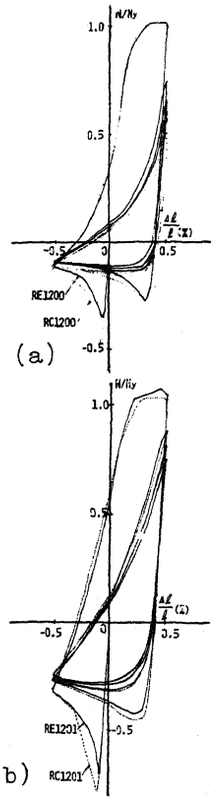

Fig.12 Influence of Eccentricity

Table 1 Test Program

NAME	ℓ(mm)	ℓ/i	ℓ/ℓ_k	e(mm)	
RC400	193	44.5	1	0.0	Square Shape
RC401	"	44.2	$\sqrt{2}$	"	
RC402	"	45.6	$\sqrt{3}$	"	
RE400	193	44.5	1	0.6	
RE401	"	44.5	$\sqrt{2}$	"	
RE402	"	44.4	$\sqrt{3}$	"	
RC800	366	84.5	1	0.0	
RC801	"	84.5	$\sqrt{2}$	"	
RC802	"	84.5	$\sqrt{3}$	"	
RE800	366	84.5	1	0.95	
RE801	"	84.5	$\sqrt{2}$	"	
RE802	"	84.4	$\sqrt{3}$	"	
RC1200	540	124.3	1	0.0	
RC1201	"	124.4	$\sqrt{2}$	"	
RC1202	"	124.1	$\sqrt{3}$	"	
RE1200	540	124.2	1	1.3	
RE1201	"	124.2	$\sqrt{2}$	"	
RE1202	"	124.4	$\sqrt{3}$	"	
RC1600	713	163.6	1	0.0	
RC1601	"	164.5	$\sqrt{2}$	"	
RC1602	"	163.8	$\sqrt{3}$	"	
HC400	232	39.6	1	0.0	H-Shape
HC401	"	39.7	$\sqrt{1.5}$	"	
HC800	464	80.4	1	0.0	
HC801	"	81.7	$\sqrt{1.5}$	"	
HC1200	696	119.4	1	0.0	
HC1201	"	120.4	$\sqrt{1.5}$	"	
HC1600	928	160.8	1	0.0	
HC1601	"	161.4	$\sqrt{1.5}$	"	

ℓ: member length, i: radius of gyration, ℓ_k: effectiv buckling length, e: eccntricity.

Table 2 Mechanical Properties

		A	B
yield stress	(t/cm²)	2.53	2.49
tensile strength	(t/cm²)	4.25	4.15
maximum elongation	(%)	33.3	30.1
strain-hardening strain	(%)	1.64	1.50

A; for square shape, B; for H-shape

DISCUSSION

S.C. Goel (U.S.A.)

Are the end restraints in experimental and theoretical models infinitely elastic ?

Author's Closure

We confirm that the end restraints in experimental and theoretical models are infinitely elastic.